

[30] Crystal data for $\text{Ce}_{60}\text{F}_{18} \cdot (\text{C}_7\text{H}_8)$, $M_r = 1154$, monoclinic, space group $P2_1/n$, $a = 11.532(2)$, $b = 21.501(3)$, $c = 16.261(2)$ Å, $\beta = 101.798(5)^\circ$, $V = 3947$ Å³, $Z = 4$, $\mu(\text{MoK}\alpha) = 0.17$ mm⁻¹, $T = 100$ K. 49263 Reflections measured (Siemens SMART diffractometer, $2\theta_{\text{max}} = 60^\circ$) 11565 unique, refined on F^2 using SHELXTL, $R1 = 0.049$ (for 6426 reflections with $I > 2\sigma(I)$), $wR2 = 0.118$ (for all reflections). Crystallographic data (excluding structure factors) for the structure reported in this paper have been deposited with the Cambridge Crystallographic Data Centre as supplementary publication no. CCDC-142291. Copies of the data can be obtained free of charge on application to CCDC, 12 Union Road, Cambridge CB21EZ, UK (fax: (+44) 1223-336-033; e-mail: deposit@ccdc.cam.ac.uk).

The First Microporous Framework Cerium Silicate**

João Rocha,* Paula Ferreira, Luís D. Carlos, and Artur Ferreira

Recently, much research has been carried out aimed at preparing inorganic microporous zeotype solids composed of interconnected octahedral- and tetrahedral-oxide polyhedra. One such family of materials of considerable interest embraces microporous titanosilicates and their derivatives which contain Ti^{IV} usually in octahedral coordination.^[1, 2] As part of a systematic search for novel microporous framework inorganic materials we have prepared (among others) AV-1, a synthetic analogue of the rare sodium yttrium silicate mineral montregianite ($\text{Na}_4\text{K}_2\text{Y}_2\text{Si}_{16}\text{O}_{38} \cdot 10\text{H}_2\text{O}$).^[3, 4] In nature, montregianite usually occurs with framework substitution of some yttrium by cerium and this raised the possibility of obtaining a purely cerous form of AV-1. Here we report the synthesis and characterization of AV-5, a microporous framework sodium cerium silicate with the structure of montregianite.

It is well known that Ce^{III} -containing materials present potential for applications in optoelectronics. For example, Ce^{III} in a LiYF_6 matrix has been shown to lase.^[5] This system may find important applications since Ce^{III} lasers emit in the high-energy region of the spectrum (blue or UV) and they exhibit tunability due to the inherently broad emission lines. Glass-supported cerium is used in Faraday rotators, which protect lasers from back-reflected light.^[6] As for other lanthanides, cerium has been used in transducers designed to detect or modify IR, UV, X-ray, and gamma radiation.^[6] The luminescence of Ce^{III} /silica systems prepared by sol-gel methods has also been studied.^[7] Our main aim with this work

was to explore the possibility of preparing porous cerium silicates with potential for use in optoelectronics.

The crystal structure of montregianite (and AV-5) consists of two different types of layers alternating along the [010] direction (Figure 1): a) a double silicate sheet, in which the

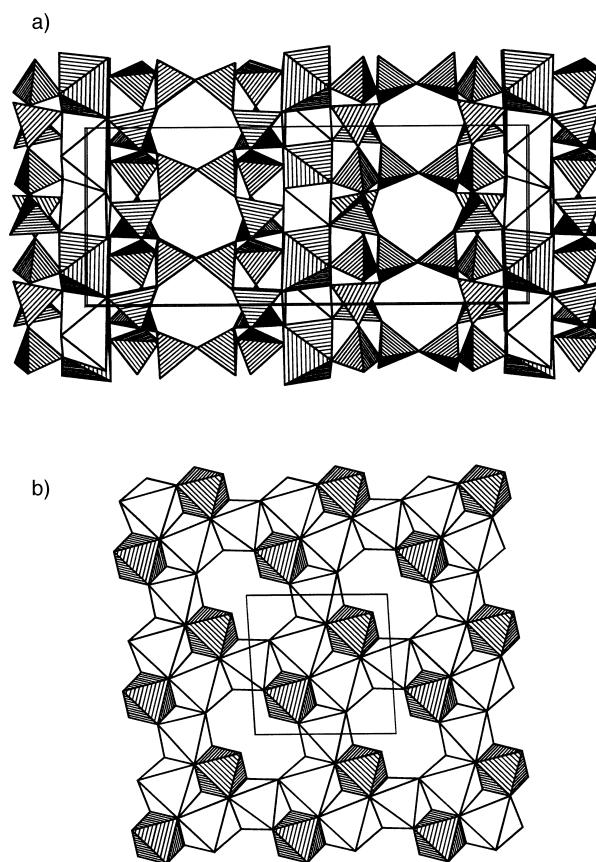


Figure 1. Polyhedral representation of the montregianite structure: a) viewed along [100] showing the alternating octahedral sheet and double silicate sheet along [010]; b) open octahedral sheet, viewed along [010], consisting of Y and three different Na^+ octahedra (unfilled octahedra).

single silicate sheet is of the apophyllite type with four- and eight-membered rings, and b) an open octahedral sheet composed of $[\text{YO}_6]$ (or $[\text{CeO}_6]$ in AV-5) and three distinct $[\text{NaO}_4(\text{H}_2\text{O})_2]$ octahedra.^[8] The layers are parallel to the (010) plane. The potassium ions are ten-coordinate and the six water molecules (not shown) are located within large channels formed by the planar eight-membered silicate rings.

Figure 2 shows the experimental and simulated powder X-ray diffraction (XRD) patterns of AV-5. The differences observed are due to the presence of a small amount of an, as-yet, unknown impurity. The unit cell parameters have been refined by assuming a monoclinic unit cell, space group $P2_1/n$, and cell dimensions $a = 9.6906(9)$, $b = 24.055(2)$, $c = 9.5759(8)$ Å, and $\beta = 93.683(7)^\circ$ and are similar to those reported for montregianite, dimensions $a = 9.512$, $b = 23.956$, $c = 9.617$ Å, and $\beta = 93.85^\circ$.^[9]

Presumably owing to the presence of paramagnetic Ce^{III} centers we were unable to record a ^{29}Si magic-angle spinning (MAS) NMR spectrum of AV-5. It is, however, possible to oxidize Ce^{III} to Ce^{IV} by calcining AV-5 in air at 300°C for 3 h.

[*] Prof. J. Rocha, Dr. P. Ferreira, A. Ferreira
Department of Chemistry
University of Aveiro
3810 Aveiro (Portugal)
Fax: (+351) 234-370084
E-mail: rocha@dq.ua.pt

Prof. L. D. Carlos
Department of Physics, University of Aveiro
3810 Aveiro (Portugal)

[**] This work was supported by PRAXIS XXI, FEDER, and FCT.

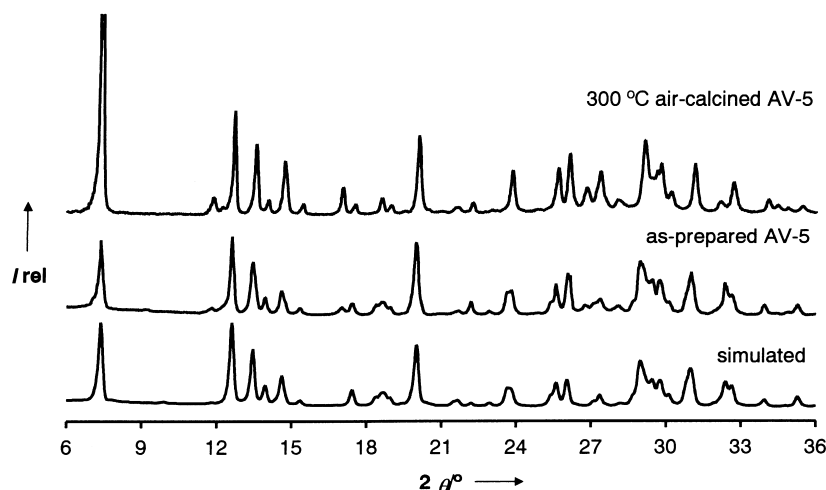


Figure 2. Experimental and simulated powder X-ray diffraction patterns of as-prepared AV-5 and 300 °C air-calcined AV-5.

In the process, the faint pink powder becomes light yellow. As shown by powder XRD (Figure 2), this treatment does not compromise the materials structural integrity. The oxidation of Ce^{III} to Ce^{IV} is accompanied by the reduction of O_2 to O^{2-} . The potassium ions which are not necessary to balance the new (less negative) AV-5 framework charge likely form an (unidentified, probably amorphous) oxide phase. The ^{29}Si MAS NMR spectrum of calcined AV-5 (Figure 3a) suggests

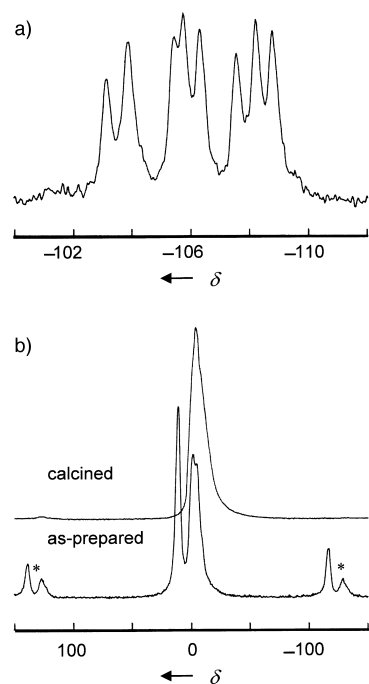


Figure 3. a) The ^{29}Si MAS NMR spectrum of as-prepared AV-5 displays eight resonance signals indicating that this solid possesses the structure of montregianite which contains an equal number of nonequivalent Si sites. The spectrum was recorded at 79.5 MHz on a Bruker MSL 400P with 45° pulses, a 5 kHz spinning rate, and 50 s recycle delays. Chemical shifts are quoted in ppm (referenced to TMS). b) Single-quantum ^{23}Na MAS NMR spectra of as-prepared and 300 °C air-calcined AV-5 recorded at 105.5 MHz with 12° pulses, 13.5 kHz spinning rates, and 2 s recycle delays. Asterisks denote spinning side bands attributed to the presence of paramagnetic Ce^{III} centers.

that AV-5 and montregianite have the same structure. Indeed, this spectrum displays eight resonance signals (deconvoluted intensities in parentheses) centered at $\delta = -103.1$ (0.9), -103.9 (1.1), -105.4 (0.9), -105.7 (1.0), -106.3 (1.1), -107.5 (1.0), -108.2 (1.1), -108.8 (1.0) in accord with the crystal structure of montregianite which reveals eight unique Si sites with equal populations. Based on the crystal structure of montregianite we attempted to assign the AV-5 ^{29}Si MAS NMR resonance signals. Two silicate tetrahedra (Si1 and Si4), one each within the four-membered rings belonging to a single sheet, have upward-pointing apices (O1) which are shared with the apices of the two downward-pointing corresponding tetrahedra (Si4 and Si1, respectively) in the second silicate sheet.^[8] Si1 and Si4 are Si(4Si) environments (Si linked to four

other Si through oxygen bridges) and the ^{29}Si MAS NMR resonance signals at $\delta = -108.8$ and -108.2 are tentatively assigned to them. The assignment of the peaks at high frequency is more difficult. Si6 is of the type Si(3Si, 1Ce). Si6–O12 is the shortest nonbridging bond length (1.562 Å in montregianite) involving the most charge-deficient oxygen atom which is bonded to a Ce atom. Considering the well known correlation between the ^{29}Si chemical shifts and the Si–O bond lengths in silicates,^[10] we tentatively assign the peak at $\delta = -107.5$ to Si6. The assignment of the other resonance signals is difficult because the NMR data available for cerium silicates is very limited.

It was possible to record a single-quantum (“conventional”) ^{23}Na MAS NMR spectrum of as-prepared AV-5. This observation immediately suggests that the solid contains some Ce^{IV} . The spectrum depicted in Figure 3b (MAS at 13.5 kHz) displays strong spinning side bands (much more so than those observed in the spectrum of synthetic montregianite) indicating the presence of Ce^{III} centers. When this spectrum is recorded with a MAS rate of 30 kHz (not shown) the prominent spinning side bands are not observed. The two central NMR resonance signals observed exhibit characteristic second-order quadrupole powder patterns centered at $\delta = 12$ and 0. The triple-quantum (3Q) MAS NMR spectrum^[11] of as-prepared AV-5 (Figure 4a) confirms that only two resonance signals are present. The AV-5 sample calcined in air at 300 °C gives a much less resolved single-quantum ^{23}Na MAS NMR spectrum (Figure 3b) and, because most Ce^{III} has been oxidized, the spinning side bands seen with MAS at 13.5 kHz (essentially due to second-order quadrupole effects) are very much fainter. The 3Q MAS NMR spectrum (Figure 4b), however, shows that two main ^{23}Na resonance signals are still present, with somewhat different quadrupole parameters. Although montregianite contains three nonequivalent sodium sites the $[\text{Na}(2\text{A})\text{O}_4(\text{H}_2\text{O})_2]$ and $[\text{Na}(2\text{B})\text{O}_4(\text{H}_2\text{O})_2]$ octahedra (populations 0.47 and 0.45, respectively) are very similar in configuration and it is unlikely that they can be distinguished by solid-state ^{23}Na NMR spectroscopy.^[3, 4, 8] The $[\text{Na}(1)\text{O}_4(\text{H}_2\text{O})_2]$ site (population 0.95) forms a weak seventh bond with O5B and is, thus, distorted. The 3Q peak S1 given

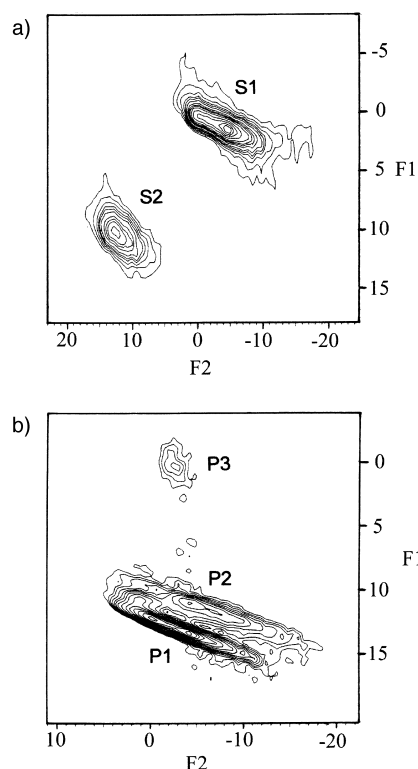


Figure 4. The unsheared 3Q ^{23}Na MAS NMR spectra of a) as-prepared and b) 300 °C air-calcined AV-5 show the presence of two main types of Na sites which are to be expected if the solids possess the structure of montregianite. A simple two-pulse sequence was used for recording the spectra.^[12] The spectrum of as-prepared AV-5 was recorded on a 2.5 mm double-bearing Bruker probe with a B_1 field amplitude of 250 kHz and a spinning rate of 30 kHz. The spectrum of the 300 °C air-calcined sample was recorded on a 4 mm double-bearing Bruker probe with a B_1 field amplitude of 125 kHz and a spinning rate of 13 kHz.

by as-prepared AV-5 displays a relatively broad powder pattern and, hence, is tentatively ascribed to the distorted NaI site. S2 is assigned to sites Na2A and Na2B. The single-quantum ^{23}Na MAS NMR spectrum of as-prepared AV-5 (Figure 3b) was simulated by assuming the presence of two resonance signals, ascribed to sites NaI and (Na2A and Na2B), with intensities of about 1:0.9 (measured from the 30 kHz MAS spectrum), respectively. The former resonance signal has an isotropic chemical shift $\delta_{\text{iso}} = 4.5$, a quadrupole coupling constant, C_Q , of 1.8 MHz, and an asymmetry parameter, η , of 0.40. The quadrupole parameters ($\delta_{\text{iso}} = 4.5$, $C_Q = 0.6\text{--}0.8$ MHz, η not determined) for the other resonance signal were estimated from the 3Q MAS NMR spectrum and used in the simulation of the single-quantum spectrum. These results are similar to those obtained previously for synthetic montregianite. The 3Q MAS NMR spectrum of AV-5 calcined at 300 °C in air (Figure 4b) exhibits, apart from the main resonance signals P1 and P2, a third faint peak P3.

The $\text{Ce}^{\text{III}}/\text{Ce}^{\text{IV}}$ conversion in AV-5 opens up several future lines of research. On one hand, controlling the amount of Ce^{III} present may be achieved by framework oxidation/reduction. For applications in the field of optoelectronics this would be important because when two Ce^{III} centers are too close the luminescence is quenched. We have carried out a preliminary luminescence study of as-prepared AV-5. Figure 5 shows the

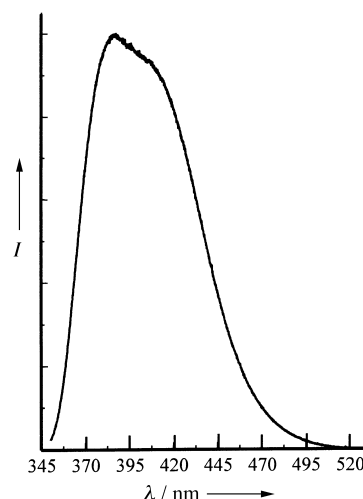


Figure 5. Emission spectrum of AV-5 recorded at 14 K. The spectrum was recorded on a 1 m spectrometer (1704 Spex) coupled to a R928 Hamamatsu photomultiplier. The 325 nm line of a He–Cd laser was used as the excitation source. The spectrum was corrected for the response of the detector.

14 K emission spectrum of this material recorded for the 325 nm He–Cd excitation line, corresponding to the main peak detected in the excitation spectrum (not shown). The blue emission observed clearly shows a broad band with two overlapping peaks centred at about 377 and about 410 nm. This is typical of Ce^{III} -activated phosphors and corresponds to transitions between the lowest Stark component of the $5d^1$ excited states and the two levels of the $4f^1$ ground state ($^2F_{5/2}$ and $^2F_{7/2}$).^[13, 14] In general, these two levels are separated by 2000 cm^{-1} , and this is indeed the result obtained by fitting the spectrum with two Gaussian lines using commercial nonlinear least-squares-fitting software. Owing to different crystal-field splitting of the 5d level the luminescence energy range strongly depends on the structure of the host crystal, varying from the near ultraviolet to the green region.^[13, 14] In the present case, the blue Ce^{III} emission is strongly dependent on the temperature (not shown). A detailed characterization of this emission is in progress.

The tuning of the adsorption properties of AV-5 is another interesting challenge. Indeed, as the Ce^{IV} content increases less channel cations are required to balance the charge of the anionic framework, thus changing the adsorption characteristics of the material. Preliminary work shows that, for example, as-prepared AV-5 calcined at 300 °C in an inert atmosphere reversibly loses and gains about 9.3 wt % water. In contrast, when heated up at 300 °C in air the material first loses 9.3 wt % but subsequent rehydration followed by calcination leads to a loss of about 15 wt %, presumably due to the oxidation of Ce^{III} to Ce^{IV} . Catalysis and ion exchange are also areas where AV-5 may find useful applications.

Experimental Section

AV-5 was prepared in Teflon-lined autoclaves under hydrothermal conditions. An alkaline solution was made by mixing sodium silicate solution (6.05 g; 27 % m/m SiO_2 , 8 % m/m Na_2O , Merck), H_2O (5.04 g), and KOH (0.91 g; Merck). A second solution was prepared by mixing $\text{Ce}_2(\text{SO}_4)_3 \cdot 8\text{H}_2\text{O}$ (1.04 g, Aldrich), H_2O (10.02 g), and HCl solution (2 M;

2.00 g). The two solutions were mixed and stirred thoroughly. The gel, with a composition $0.29\text{Na}_2\text{O}:0.30\text{K}_2\text{O}:1.0\text{SiO}_2:0.054\text{Ce}_2\text{O}_3:34.8\text{H}_2\text{O}$, was placed in an autoclave for eight days at 230°C . The crystalline product was filtered, washed with distilled water, and dried at ambient temperature. Bulk chemical analysis (ICP) yielded an Si/Ce/(Na + K) ratio of 8.6:1.0:2.3. The Si/Ce molar ratio of 8.6:1 is slightly larger than expected assuming a montregianite-type structure for which Si/Ce = 8:1. This is partially due to the presence of some amorphous siliceous phase. Indeed, the baseline of the ^{29}Si MAS NMR spectrum is slightly raised, although (due to the horizontal expansion) this is not clearly seen in Figure 3a. In addition, powder X-ray diffraction exhibits faint reflections from unknown impurities, while scanning electron microscopy (SEM) shows the presence of some poorly defined particles of very small size. The (Na + K)/Ce ratio of 2.3:1 is between 2 and 3, as expected for samples containing only Ce^{IV} or Ce^{III} , respectively. The K/Na ratio is 0.4:1.

Although small (40 μm at best) some of the AV-5 crystals seemed to be of good quality. It was, however, not possible to solve the structure by single-crystal methods. The sample was ground prior to data collection for Rietveld refinement. Powder XRD data were collected on a X'Pert MPD Philipps diffractometer ($\text{CuK}\alpha$ radiation) with a curved graphite monochromator, constant slit, and a flat plate sample holder, in a Bragg-Brentano para-focusing optics configuration. Different grinding times were used and several data sets obtained. The unit cell parameters were first obtained with program TREOR90.^[15] The Rietveld refinement was carried out with program Fullprof,^[16] in the space group $P2_1/n$, range $5-100\ 2\theta$, using the atomic coordinates of montregianite and assuming full Ce for Y substitution. The background, peak shapes, and cell parameters were refined. The refinement reliability factors were relatively poor ($R_p = 0.138$, $R_{wp} = 0.177$), probably due to the presence of unknown impurities and to orientation effects.

Received: August 30, 1999

Revised: May 18, 2000 [Z13937]

- [1] S. M. Kuznicki, US-A 4,853,202, **1989**.
- [2] M. W. Anderson, O. Terasaki, T. Ohsuna, A. Phillippou, S. P. Mackay, A. Ferreira, J. Rocha, S. Lidin, *Nature* **1994**, 367, 347–351.
- [3] J. Rocha, P. Ferreira, Z. Lin, P. Brandão, A. Ferreira, J. D. Pedrosa de Jesus, *Chem. Commun.* **1997**, 2103–2104.
- [4] J. Rocha, P. Ferreira, Z. Lin, P. Brandão, A. Ferreira, J. D. Pedrosa de Jesus, *J. Phys. Chem. B* **1998**, 102, 4739–4744.
- [5] D. J. Ehrlich, P. F. Moulton, R. M. Osgood, *Opt. Lett.* **1980**, 5, 339.
- [6] R. Reisfield, *Inorg. Chim. Acta* **1987**, 140, 345.
- [7] E. R. Rhand, M. B. Smuckler, E. Go., M. S. Bradley, J. W. Bruno, *Inorg. Chim. Acta* **1995**, 233, 71.
- [8] S. Ghose, P. K. S. Gupta, C. F. Campana, *Am. Mineral.* **1987**, 72, 365.
- [9] G. Y. Chao, *Can. Mineral.* **1978**, 16, 561.
- [10] G. Engelhardt, D. Michel, *High-Resolution Solid-State NMR of Silicates and Zeolites*, Wiley, New York, **1987**.
- [11] A. Medek, J. S. Hardwood, L. Frydman, *J. Am. Chem. Soc.* **1995**, 117, 12779–12787.
- [12] C. Fernandez, J. P. Amoureux, J. M. Chezeau, L. Delmotte, H. Kessler, *Microporous Mater.* **1996**, 6, 331–340.
- [13] G. Blasse, B. C. Grabmaier, *Luminescent Materials*, Springer, Berlin, **1994**, pp. 45–47.
- [14] T. Kano, *Phosphor Handbook*, (Eds.: S. Shionoya, W. M. Yen), CRC press, Boca Raton, **1998**, 186–188.
- [15] P. E. Werner, L. Eriksson, M. Westdahl, *J. Appl. Crystallogr.* **1985**, 18, 367–370.
- [16] J. R.-Carvajal, *Collected Abstract of Powder Diffraction Meeting*, Toulouse, France, **1990**, p. 127.

Is Hydrogen Tunneling Involved in AcylCoA Desaturase Reactions? The Case of a Δ^9 Desaturase That Transforms (*E*)-11-Tetradecenoic Acid into (*Z,E*)-9,11-Tetradecadienoic Acid**

José Luís Abad, Francisco Camps, and Gemma Fabriàs*

Introduction of double bonds into the unactivated aliphatic chains of fatty acids is one of the most remarkable transformations in living organisms. This reaction is catalyzed by specific desaturases, which are oxygen-dependent enzymes containing a non-heme diiron cluster at their active site.^[1] The mechanism of enzymatic desaturation of fatty acids is a subject of currently active research. It has been proposed^[2–5] that desaturation reactions begin with an initial hydrogen atom abstraction step by a hypervalent iron–oxo species to generate a very short lived intermediate, that is then transformed into the olefin via a one-electron oxidation/deprotonation or simple disproportion process. Large activation energies are required to cleave the stable C–H bonds in the substrates as the first step of desaturation. How the enzyme manages to perform such a difficult reaction is an interesting question and the contribution of hydrogen tunneling (H-tunneling) is an attractive possibility. It has been proposed^[2, 3] that enzymatic desaturation and hydroxylation of unactivated aliphatic chains do share common mechanistic features and H-tunneling has been invoked in the oxidation of linoleic acid catalyzed by soybean lipoxygenase.^[6] H-tunneling is defined as a phenomenon by which an atom transfers through a reaction barrier as a result of its wave-like properties.^[7] Reports that show H-tunneling in enzymes are relatively recent.^[7–9] This is an important event in enzyme catalysis, since it contributes to circumvent the thermodynamic difficulties associated with classical descriptions of C–H bond cleavage.

To investigate the putative effect of hydrogen tunneling in fatty acid desaturase reactions, we report herein on a mechanistic study on one of these catalysts, namely the Δ^9 desaturase of (*E*)-11-tetradecenoic acid,^[10] using the moth *Spodoptera littoralis* as biological model.

To determine the cryptoregiochemistry or initial oxidation site of the reaction, the same methodology previously validated for other desaturases^[3–5, 11] was followed. This procedure is based on the calculation of intermolecular, primary kinetic isotope effects (KIE) in competitive experi-

[*] Dr. G. Fabriàs, Dr. J. L. Abad, Prof. Dr. F. Camps
Department of Biological Organic Chemistry (IIQAB-CSIC)
Jordi Girona 18-26, 08034 Barcelona (Spain)
Fax: (+34) 93-204-5904
E-mail: gfdqob@cid.csic.es

[**] This work was supported by Comisión Asesora de Investigación Científica y Técnica (grant AGF 98-0844), Comissionat per a Universitats i Recerca from the Generalitat de Catalunya (grant 97SGR-0021) and SEDQ S.A. We thank Prof. Nigel S. Scrutton (University of Leicester, UK) and Dr. Francisco J. Sanchez-Baeza (IIQAB, Barcelona, Spain) for helpful discussions, Dr. Josefina Casas and Dr. Antonio Delgado for critically reading the manuscript, and Germán Lázaro for rearing the insects used in this study. J.L.A. thanks the Spanish Ministry of Education and Science for a Postdoctoral Reincorporation Contract.